Carbon

DOI: 10.1002/anie.201402513

Room-Temperature Carbide-Derived Carbon Synthesis by Electrochemical Etching of MAX Phases**

*Maria R. Lukatskaya, Joseph Halim, Boris Dyatkin, Michael Naguib, Yulia S. Buranova, Michel W. Barsoum, and Yury Gogotsi**

Abstract: *Porous carbons are widely used in energy storage and gas separation applications, but their synthesis always involves high temperatures. Herein we electrochemically selectively extract, at ambient temperature, the metal atoms from the ternary layered carbides, Ti_3AlC_2, Ti_2AlC and Ti_3SiC_2 (MAX phases). The result is a predominantly amorphous carbide-derived carbon, with a narrow distribution of micropores. The latter is produced by placing the carbides in HF, HCl or NaCl solutions and applying anodic potentials. The pores that form when Ti_3AlC_2 is etched in dilute HF are around 0.5 nm in diameter. This approach forgoes energy-intensive thermal treatments and presents a novel method for developing carbons with finely tuned pores for a variety of applications, such as supercapacitor, battery electrodes or CO_2 capture.*

Carbon materials with various dimensions offer extraordinarily high structural versatility and significant promise in numerous applications. Along with fundamentally interesting 0D, 1D, and 2D allotropes, such as fullerenes, nanotubes and graphene, 3D porous carbon architectures are useful in many emerging energy related applications,[1,2] such as battery anodes, electrode materials for supercapacitors, and catalyst supports in fuel cells.[2–6] In addition to their high surface areas and high conductivity, porous carbons are environmentally benign and show many attractive properties.[1,7–9] Among those, activated and templated carbons are the most widely studied, but carbide-derived carbons (CDCs) produced by the thermal or thermochemical removal of metals from carbides have received much attention in the past decade. This method yields carbon materials with highly tunable porosities and surface areas,[10] electric properties,[11] and surface chemistries.[12]

The most common method to produce CDCs uses selective etching of metalloid atoms (Ti, Si, etc.) from binary or ternary carbides using chlorine gas (Cl_2). Volatile chlorides are removed with the gas flow, leaving behind a porous CDC.[10] While this process is effective, it requires the use of Cl_2 gas that leaves traces of metal chlorides that may affect biocompatibility or cause corrosion, and can only be done at temperatures of 200 °C or higher. Several chlorine-free alternative approaches to CDC synthesis—such as vacuum decomposition at high temperatures[13,14] or hydrothermal treatment of carbides[15–18]—have been demonstrated. Notably, synthesis of CDCs at room temperature, except for recently reported nanometer-thin films on SiC[19] has remained elusive.

A decade ago, it was shown that CDCs can be produced by Cl_2 etching of the MAX phases.[20–22] The latter are so called because their general formula is $M_{n+1}AX_n$ ($n = 1, 2, 3$), where M represents an early transition metal, A mostly represents IIIA or IVA group elements, and X represents either C or/and N. The MAX phases are inherently nanolayered (Figure 1 a). The bonding between the A and M layers

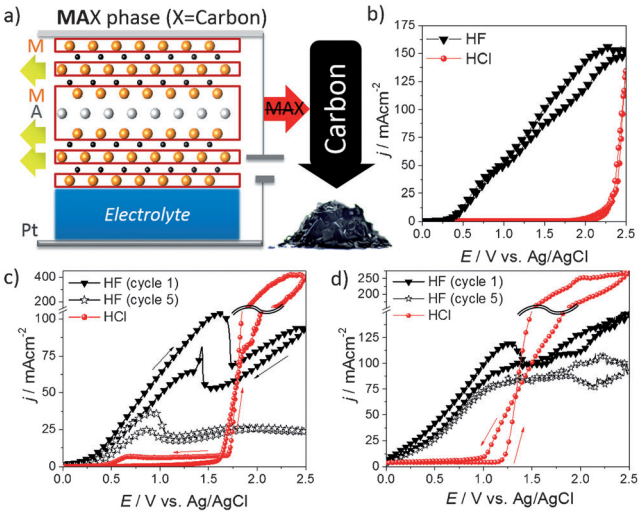

Figure 1. a) Schematic representation of the room-temperature CDC synthesis from MAX phase. b–d) Cyclic voltammograms obtained in HF (green) and HCl (circles) when, b) Ti_3SiC_2, c) Ti_3AlC_2, and d) Ti_2AlC were used as anodes. For the case of HF, cycles 1 (triangles) and 5 (stars) are shown.

is relatively weak compared to the M–X bonds that are quite similar to the bonds in their binary MX counterparts, i.e. strong, mixed metallic–ionic–covalent.[22] CDCs produced from MAX phases have shown significant promise as materials for energy storage, catalyst support, water filtration, and several biomedical applications.[9,10,23,24]

Herein the working hypothesis was that, since the MAX phases possess metallic-type conductivity, they may be good

[*] M. R. Lukatskaya, J. Halim, B. Dyatkin, M. Naguib, Y. S. Buranova,[+] Prof. M. W. Barsoum, Prof. Y. Gogotsi
A. J. Drexel Nanomaterials Institute, and Materials Science and Engineering Department, Drexel University
3141 Chestnut Street, Philadelphia, PA 19104 (USA)
E-mail: gogotsi@drexel.edu
[+] Current address: Institut für Materialphysik
Westfälische Wilhelms-Universität Münster (Germany)

[**] This work was supported by the U.S. Department of Energy, Office of Science, Basic Energy Sciences, under Award no. ER46473.
Supporting information for this article is available on the WWW under http://dx.doi.org/10.1002/anie.201402513.

candidates for anodic de-alloying.[25] The purpose of this paper is to report on the room temperature electrochemical conversion of three MAX phases—Ti_3AlC_2, Ti_2AlC and Ti_3SiC_2—into CDCs. Three aqueous solutions (5 wt.% NaCl; 10 wt.% HCl; and 5 wt.% HF) were used as electrolytes. A general schematic of the synthesis concept is depicted in Figure 1a. By the application of an anodic potential at room temperature, the M and A elements are selectively etched, resulting in the formation of a predominantly amorphous CDC, with a narrow pore size distribution.

To explore the effect of the A-group element on anodic de-alloying, Ti_3SiC_2 and Ti_3AlC_2 were compared. To investigate the effect of n, Ti_3AlC_2 and Ti_2AlC were compared. All samples were initially fully dense and predominantly single-phase.

The cyclic voltammograms (CVs) obtained when these phases were tested in the acidic solutions are shown in Figure 1b–d. In the case of Ti_3SiC_2 in HF (Figure 1b), active dissolution was observed at potentials >0.5 V (vs. Ag/AgCl). Only pitting corrosion occurred in HCl, accompanied by gas evolution, at potentials >2.0 V (Figure 1b). Whereas peaks were observed in the CVs of the Ti_3AlC_2 (Figure 1c) and Ti_2AlC samples (Figure 1d). Based on these peaks, it is reasonable to conclude that etching of the latter is a 2-step process: first, the removal of Al, and then both Al and Ti atoms depending on the magnitude of the positive potential(Figure 1c,d). Except for the Ti_3SiC_2 sample etched in HCl, in all other cases, including etching in 5 wt.% NaCl (see CV in Figure S1 in the Supporting Information (SI)), the treatments resulted in the formation of black films on the MAX phases' surfaces. The films produced by etching of Ti_3AlC_2 in HF and HCl were further characterized in detail. Based on the similarity of the morphologies of the films formed on the other MAX phases, it is reasonable to assume that the latter are quite similar.

Transmission electron microscope (TEM) micrographs of the Ti_3AlC_2 sample that was partially etched in HF are shown in Figure 2. Energy-dispersive spectroscopy (EDS) confirmed the absence of Ti and Al, leaving behind only carbon. This is best seen in Figure 2a,b, where, at their edges, the MAX layers are converted to carbon. For the most part, the carbon was amorphous (Figure 2d) as confirmed by X-ray diffraction (Figure S2) and Raman spectra showing broad D and G bands of graphitic carbon (Figure 3a and S3, Table S1). Some regions contained ordered carbon (Figure 2c). The films, however, were mostly comprised of amorphous carbon. Thermogravimetric analysis (SI, Section 6, Figure S5) of the collected films in air showed that the onset of oxidation occurred at relatively low temperatures.

In addition to carbon, EDS and X-ray photoelectron spectroscopy (XPS) showed the presence of a high concentration of oxygen (SI, Section 5). In other words, it appears that the CDC surfaces are functionalized by oxygen and OH. The CDC films produced after Ti_3AlC_2 was etched in 5 wt.% HF solution were comprised of 20 at.% O and 80 at.% C, according to EDS. XPS elemental analysis of the CDC produced by electrochemical etching of Ti_3AlC_2 in HCl and HF is summarized in Tables S2 and S3, respectively.

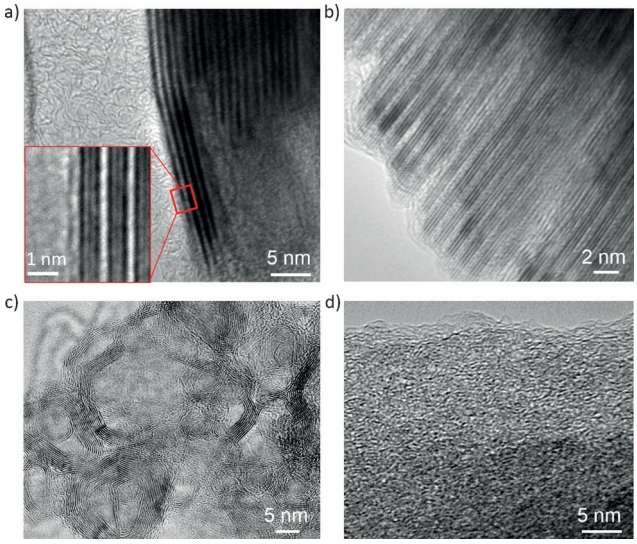

Figure 2. TEM micrographs of CDCs produced by electrochemical etching of Ti_3AlC_2 in 5 wt.% HF. a) CDC/Ti_3AlC_2 interface region. Inset shows a higher magnification of the area confined by the rectangle. b) Same as (a) but at a higher magnification. c) Ordered and d) amorphous CDC structures.

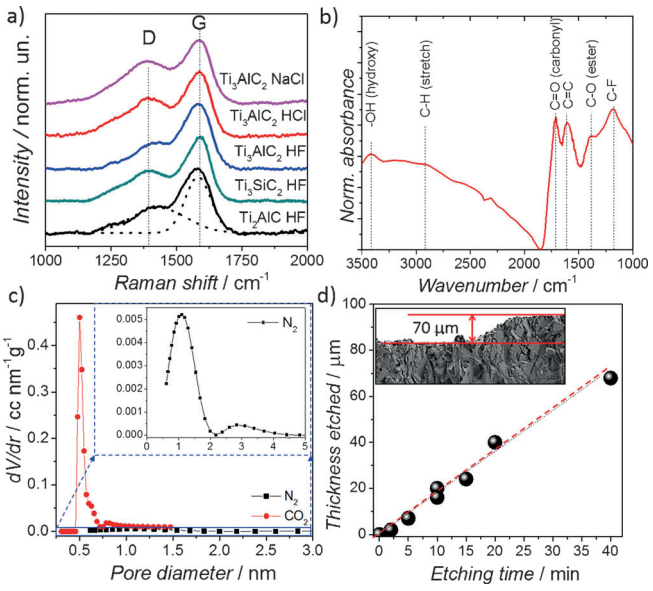

Figure 3. Characterization of electrochemically produced CDC. a) Raman spectra of select carbon synthesized from Ti_3SiC_2, Ti_3AlC_2, and Ti_2AlC in HF and Ti_3AlC_2 in HCl and NaCl electrolytes. b) FTIR spectra of Ti_3AlC_2-CDC. c) Pore size distribution for the Ti_3AlC_2 CDC obtained by CO_2 and N_2 gas sorption (inset). d) Time-dependence of etched thickness for Ti_3AlC_2 sample etched in 5 wt.% HF at a constant current of 100 mA cm^{-2}. Inset: SEM image of the etching profile.

Analysis of high-resolution C1s and O1s XPS spectra (Tables S4 and S5) suggests that the major constituents are carbon atoms bonded to either C or O atoms for CDCs produced from Ti_3AlC_2 in HCl or HF. In the HCl case, the ratio of C–C bonds to C–O is ca. 2.5; in HF case, the ratio is ca. 4.3.

Fourier transform infrared spectroscopy (FTIR) analysis of CDCs produced by etching Ti_3AlC_2 in HF (Figure 3b) shows that the surface becomes terminated with -C=O, -OH, and other similar groups that form in the aqueous environment during synthesis. Not surprising, those terminations are similar to those deduced from XPS peak analysis of the C1s and O1s regions (see Figure S4 and Table S5). A prominent C–F peak (at 1100 cm^{-1}) also suggests that some carbon atoms are terminated with fluorine. This is similar to halide bonds found on the surfaces of CDCs prepared by high-temperature halogen etching.[12] We were unable to fit the F region in XPS due to its low intensity and low (< 0.5 at.%) nominal fluorine content in the sample.

Porosity calculations derived from N_2 and CO_2 sorption measurements on CDCs produced from etching Ti_3AlC_2 in HF showed a very narrow pore size distribution, with a sharp peak at 0.5 nm (Figure 3c, additional details can be found in SI, Section 2). At the low synthesis temperatures used here, the mobility of C atoms is probably too low to allow the CDC structure to significantly transform, which partially explains why the pores are as small as they are. This is consistent with previous work on the low-temperature synthesis of CDCs.[26]

To quantify the etching kinetics, a series of experiments were carried out on Ti_3AlC_2 in HF. In these experiments, a portion of a mirror-finished Ti_3AlC_2 surface was covered by an adhesive tape. Galvanostatic experiments, with a current densities of 100 mA cm^{-2}, were then carried out for different time intervals. After each etching, the C layer was detached from the substrate and the profiles were analyzed using SEM imaging of fractured surfaces (inset in Figure 3d). When the resulting time dependencies of the thicknesses were plotted (Figure 3d) a straight line that goes through the origin was obtained signifying that the kinetics are linear and thus the process is most probably interfacial reaction rate controlled and is thus highly scalable. For example, based on Figure 3d, 50 μm of Ti_3AlC_2 can be converted to a CDC film in about 30 min.

In conclusion, room-temperature electrochemical anodic etching of the select MAX phases in dilute HF, HCl and NaCl solutions resulted in the synthesis of the CDCs with high rates. This finding opens a novel route for the room-temperature synthesis of porous carbons. Similar to higher-temperature chlorine etching, this method allows us to produce thick carbon films.[27] Unlike halogen synthesis, however, this new method is carried out under ambient conditions and electrochemistry is used instead of Cl_2 gas to extract the metals. CDC patterns can be obtained by partial masking of the carbide surface. It is important to note that much like traditional CDC materials, theoretical carbon yield is on the order of 10–20% (weight percentage of carbon in the carbide structure). Exact calculations for the theoretical carbon yield from Ti_3SiC_2, Ti_3AlC_2, Ti_2AlC can be found in SI, Section 8. A wide variety of electrically conductive ternary carbides from the MAX phase family can be used as precursors and synthesis procedures can be tuned to achieve the required structures optimized for specific applications. These efforts may, for example, increase the accessible surface areas yet retain the narrow pore size distributions, making these materials highly attractive for a number of research and commercial applications.

The extremely small pore size of the synthesized carbon makes it particularly attractive for hydrogen and CO_2 storage.[28] Apart from gas separation or storage applications[29] such materials could be used in tribology[30] or electrical energy storage[3,5,31] among others, where CDCs produced by chlorine etching of metal carbides have shown excellent performance. It is reasonable to assume that these CDCs can also be used in capacitive energy storage applications, where narrow pore size distributions matter.[9] Studying the properties and performance of this new form of CDCs is the next frontier.

Experimental Section

Cyclic voltammograms (CVs) in the various electrolytes were recorded in a 3-electrode cell where the MAX phase was the working electrode, Ag/AgCl in 3 M NaCl was the reference electrode, and Pt mesh was the counter electrode. The cycling rate in all cases was 5 mV s^{-1}. All CDC samples used for structural and compositional characterization were obtained by galvanostatic etching using a constant current density of 100 mA cm^{-2}. Detailed information about the characterization techniques used and the MAX phase sample preparation procedures can be found in the Supporting Information.

Received: February 17, 2014
Published online: April 1, 2014

Keywords: carbides · carbon · cyclic voltammetry · electrochemistry · oxidation

[1] Y. Gogotsi, V. Presser, *Carbon Nanomaterials*, 2nd ed., CRC, Boca Raton, **2013**.
[2] F. Béguin, E. Frackowiak, *Carbons for Electrochemical Energy Storage and Conversion Systems*, CRC, Boca Raton, **2010**.
[3] Y. Zhai, Y. Dou, D. Zhao, P. F. Fulvio, R. T. Mayes, S. Dai, *Adv. Mater.* **2011**, *23*, 4828 – 4850.
[4] A. L. Dicks, *J. Power Sources* **2006**, *156*, 128 – 141.
[5] Q. Lu, J. G. Chen, J. Q. Xiao, *Angew. Chem.* **2013**, *125*, 1932 – 1940; *Angew. Chem. Int. Ed.* **2013**, *52*, 1882 – 1889.
[6] M. Oschatz, L. Borchardt, M. Thommes, K. A. Cychosz, I. Senkovska, N. Klein, R. Frind, M. Leistner, V. Presser, Y. Gogotsi, S. Kaskel, *Angew. Chem.* **2012**, *124*, 7695 – 7698; *Angew. Chem. Int. Ed.* **2012**, *51*, 7577 – 7580.
[7] Z. Yang, J. Zhang, M. C. Kintner-Meyer, X. Lu, D. Choi, J. P. Lemmon, J. Liu, *Chem. Rev.* **2011**, *111*, 3577 – 3613.
[8] M. He, Y. Sun, B. Han, *Angew. Chem.* **2013**, *125*, 9798 – 9812; *Angew. Chem. Int. Ed.* **2013**, *52*, 9620 – 9633.
[9] W. Gu, G. Yushin, *Wiley Interdiscip. Rev. Energy Environ.* **2013**, DOI: 10.1002/wene.102.
[10] V. Presser, M. Heon, Y. Gogotsi, *Adv. Funct. Mater.* **2011**, *21*, 810 – 833.
[11] P. M. Vora, P. Gopu, M. Rosario-Canales, C. R. Perez, Y. Gogotsi, J. J. Santiago-Aviles, J. M. Kikkawa, *Phys. Rev. B* **2011**, *84*, 155114.
[12] C. Portet, D. Kazachkin, S. Osswald, Y. Gogotsi, E. Borguet, *Thermochim. Acta* **2010**, *497*, 137 – 142.
[13] Z. G. Cambaz, G. Yushin, S. Osswald, V. Mochalin, Y. Gogotsi, *Carbon* **2008**, *46*, 841 – 849.
[14] A. Jänes, T. Thomberg, E. Lust, *Carbon* **2007**, *45*, 2717 – 2722.
[15] R. Roy, D. Ravichandran, A. Badzian, E. Breval, *Diamond Relat. Mater.* **1996**, *5*, 973 – 976.

[16] Y. G. Gogotsi, M. Yoshimura, *Nature* **1994**, *367*, 628 – 630.
[17] N. S. Jacobson, Y. G. Gogotsi, M. Yoshimura, *J. Mater. Chem.* **1995**, *5*, 595 – 601.
[18] K. Byrappa, M. Yoshimura, *Handbook of Hydrothermal Technology*, Access Online via Elsevier, **2001**.
[19] J. Senthilnathan, C.-C. Weng, W.-T. Tsai, Y. Gogotsi, M. Yoshimura, *Carbon* **2014**, *71*, 181 – 189.
[20] M. W. Barsoum, M. Radovic, *Encyclopedia of Materials*: *Science and Technology*, 2nd ed. (Eds.: K. H. J. Buschow, R. Cahn, M. C. Flemings, B. Ilschner, E. J. Kramer,S. Mahajan), Elsevier, Oxford, **2004**, pp. 1 – 16.
[21] P. Eklund, M. Beckers, U. Jansson, H. Högberg, L. Hultman, *Thin Solid Films* **2010**, *518*, 1851 – 1878.
[22] M. W. Barsoum, *MAX Phases*: *Properties of Machinable Ternary Carbides and Nitrides*, Wiley-VCH, Weinheim, **2013**.
[23] J. Eskusson, A. Jänes, A. Kikas, L. Matisen, E. Lust, *J. Power Sources* **2011**, *196*, 4109 – 4116.
[24] G. Yushin, E. N. Hoffman, M. W. Barsoum, Y. Gogotsi, C. A. Howell, S. R. Sandeman, G. J. Phillips, A. W. Lloyd, S. V. Mikhalovsky, *Biomaterials* **2006**, *27*, 5755 – 5762.
[25] V. D. Jovic, B. M. Jovic, S. Gupta, T. El-Raghy, M. W. Barsoum, *Corros. Sci.* **2006**, *48*, 4274 – 4282.
[26] G. N. Yushin, E. N. Hoffman, A. Nikitin, H. Ye, M. W. Barsoum, Y. Gogotsi, *Carbon* **2005**, *43*, 2075 – 2082.
[27] D. A. Ersoy, M. J. McNallan, Y. Gogotsi, *Mater. Res. Innovations* **2001**, *5*, 55 – 62.
[28] Y. Gogotsi, C. Portet, S. Osswald, J. M. Simmons, T. Yildirim, G. Laudisio, J. E. Fischer, *Int. J. Hydrogen Energy* **2009**, *34*, 6314 – 6319.
[29] E. Kockrick, C. Schrage, L. Borchardt, N. Klein, M. Rose, I. Senkovska, S. Kaskel, *Carbon* **2010**, *48*, 1707 – 1717.
[30] B. Carroll, Y. Gogotsi, A. Kovalchenko, A. Erdemir, M. J. McNallan, *Tribol. Lett.* **2003**, *15*, 51 – 55.
[31] J. Chmiola, C. Largeot, P.-L. Taberna, P. Simon, Y. Gogotsi, *Angew. Chem.* **2008**, *120*, 3440 – 3443; *Angew. Chem. Int. Ed.* **2008**, *47*, 3392 – 3395.

